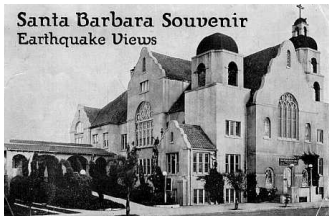

4th IASPEI / IAEE International Symposium:

Effects of Surface Geology on Seismic Motion

August 23–26, 2011 · University of California Santa Barbara

A COMPARISON OF AMPLITUDES OF NOISE CORRELATION MEASUREMENTS

Victor C. Tsai
Seismological Laboratory
California Institute of Technology
Pasadena, CA 91125
USA

ABSTRACT

Cross correlations of ambient seismic noise have been used to produce both travel time and attenuation maps. However, while there is currently good understanding of what affects the travel times of noise correlation measurements, theory to understand the amplitudes has just begun to be worked out. Here we utilize the ray-theory framework of Tsai (2011), which accounts for attenuation and the spatial distribution of noise sources, and evaluate the effect of various noise source distributions on the decay of amplitudes with station-station distance. We quantify the amplitudes of coherency measurements for four specific noise source distributions that are relatively simple. These examples show that coherency amplitudes depend on noise source distributions in a predictable way. We therefore suggest that attenuation measurements can be made from noise coherency if one first approximately determines how the dominant sources of noise are distributed, and if data are chosen properly.

INTRODUCTION

Ambient noise tomography has been a popular imaging technique ever since Shapiro et al. (2005) first showed that the method could produce high-resolution tomographic images. While most of the work to date using ambient noise methods has focused on travel times, there have been recent efforts to use the amplitudes of ambient noise correlations to perform attenuation tomography (Prieto et al. 2009; Lawrence and Prieto 2011; Lin et al. 2011). While the accuracy of travel-time noise correlation measurements is well understood (Cox 1973; Tsai 2009; Harmon et al. 2010), only preliminary work has been done to understand the accuracy of attenuation measurements when noise sources are distributed non-uniformly in space (Tsai 2011). In this work, we extend some of the results of Tsai (2011) to a few cases that are still relatively simple but are perhaps more realistic.

NOISE CORRELATION THEORY

The basic theory for understanding both the amplitudes and travel times of noise correlation measurements for surface waves has been laid out by Tsai (2011). For completeness, we summarize some of the key results here. We take $u(\mathbf{x},t)$ to be a single displacement component observed at location $\mathbf{x}$ and time t, assume that u satisfies the damped wave equation in two dimensions (2D), and that there exist a spatial distribution of noise sources $A(\mathbf{x},\omega)$ that can be frequency (ω) dependent. With the further assumption that only coherent terms contribute energy, the cross correlation is given by

$$C_{xy}(t) = \Re\left[\int_0^{\infty}\int_0^{2\pi} rA^2(r,\theta)e^{-\alpha(r_- + r_+)}H_0^{(1)}\left(\frac{\omega r_+}{c}\right)H_0^{(2)}\left(\frac{\omega r_-}{c}\right)e^{-i\omega t}\,d\theta\,dr\right] \quad (1)$$

where $\Re$[f] denotes the real part of f, α is the (frequency-dependent) attenuation coefficient, c is the (frequency-dependent) phase

velocity, $H_k^{(j)}$ are Hankel functions of the first (j=1) and second (j=2) kind, of order k, and $r_{\pm} = \sqrt{r^2 + r_{xy}^2/4 \pm r r_{xy}\cos\theta}$, where r_{xy} is the distance between locations x and y. Cross correlation results for different distributions of noise sources, $A(r,\theta)$, can then be evaluated simply by integration of Eq. (1). In certain simple cases, analytic expressions can be derived for C_{xy} whereas in most cases, one must resort to numerical calculation.

One approach to measuring attenuation is to examine the amplitudes of the normalized cross correlation, or coherency (Prieto 2009). This normalized cross correlation is often treated in the frequency domain and can be expressed as

$$\hat{C}_{xy}(\omega) = \frac{C_{xy}(\omega)}{\sqrt{C_{xx}(\omega)C_{yy}(\omega)}}, \tag{2}$$

where $C_{xy}(\omega)$ is the Fourier transform of $C_{xy}(t)$ (Tsai 2011).

COHERENCY RESULTS FOR EXAMPLE NOISE DISTRIBUTIONS

As noted above, cross correlation (and coherency) results can only be obtained analytically in certain simple cases. In the remainder of cases, numerical calculations must be done. Here, we first summarize a few key analytic results and then show a few key numerical results. A schematic of the different noise distributions considered is shown in Fig. 1.

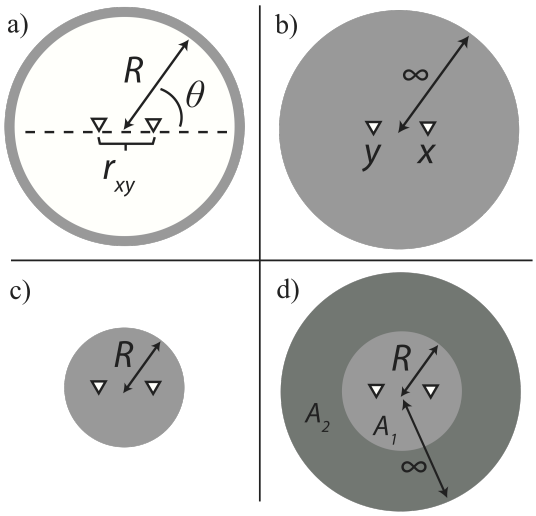

Fig. 1. Schematic noise source distributions considered. Source density is shown in grayscale.

Analytic Results

Tsai (2011) showed a number of simple cases in which Eq. (1) can be integrated analytically. The five primary source distributions examined were (1) uniform far-field, (2) one-sided uniform far-field, (3) arbitrary far-field, (4) uniform in whole plane, and (5) uniform near-field. Expressions for the coherency in cases (1), (4) and (5) are summarized here. In case (1),

$$\hat{C}_{xy}(\omega) = \frac{1}{I_0(\alpha r_{xy})} J_0\left(\frac{\omega r_{xy}}{c}\right), \tag{3}$$

where $J_k(x)$ is a Bessel function of the first kind, of order k, and $I_k(x)$ is a modified Bessel function of the first kind, of order k. In case (4),

$$\hat{C}_{xy}(\omega) = e^{-\alpha r_{xy}} J_0\left(\frac{\omega r_{xy}}{c}\right), \tag{4}$$

and has the exponential decay with distance expected of the Green's function response. In case (5), the coherency is approximately given by

$$\hat{C}_{xy}(\omega) = \sqrt{1 - \frac{r_{xy}^2}{4R^2}} \cdot J_0\left(\frac{\omega r_{xy}}{c}\right), \tag{5}$$

where R is the size of the circular region surrounding the stations that is uniformly covered with noise sources, we have set $\alpha=0$, and it is assumed that $R>r_{xy}/2$ (when this inequality is not satisfied, the coherency is expected to be approximately zero). (See Tsai (2011) for more discussion of the approximations used here.) One may observe that Eqs. (3), (4) and (5) all have the phases and geometrical spreading expected of the Green's function response (the J_0 term) but only Eq. (4) has the attenuation response expected of the Green's function (the exponential term). The Green's function phases are expected since all three of the distributions are azimuthally uniform. (A non-uniform azimuthal distribution would not be expected to have the same phases.) The non-J_0 parts of Eqs. (3), (4) and (5) are plotted in Fig. 2.

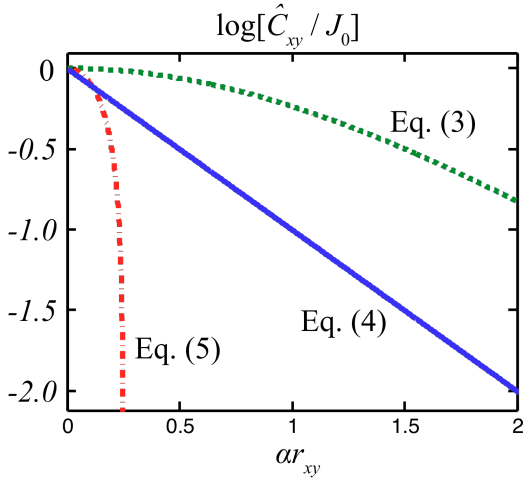

Fig. 2. Decay of coherency beyond the J_0 term for Eqs. (3) (dashed green), (4) (solid blue) and (5) (dot-dashed red).

Numerical Results

In this study, we show numerical results only for a hybrid uniform near-field plus uniform far-field situation, as shown in Fig. 1d, with $A=A_1$ interior to $r=R$ and $A=A_2$ exterior to $r=R$. We take representative values for parameters to be $c=3$ km/s, $\omega=2\pi/10$ s (period is 10 s), and $\alpha=2\cdot10^{-3}$/km (Prieto 2009). We further assume that $R=200$ km, that r_{xy} varies continuously from 0 to 200 km, and that the ratio of $\rho\equiv A_2^2/A_1^2$ takes values of 0, 1, 3, 9 or ∞. (Note that when $r_{xy}=200$ km, the stations are still 100 km away from the exterior/interior boundary.) The non-J_0 parts of the numerically computed coherencies are plotted in Fig. 3. Numerical integration is performed with an adaptive Gauss-Kronrod rule.

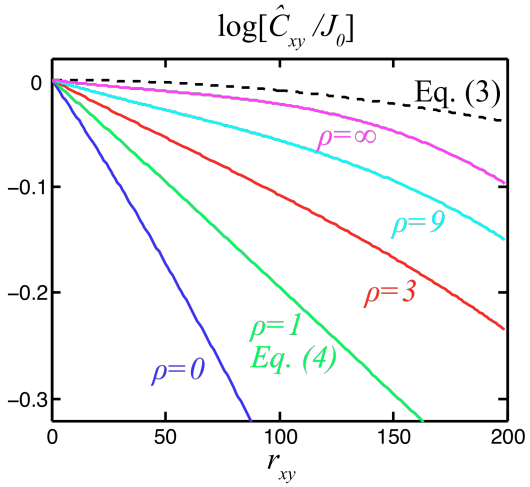

Fig. 3. Decay of coherency beyond the J_0 term for ρ=0 (blue), 1 (green), 3 (red), 9 (cyan), and ∞ (magenta). The ρ=1 curve is identical to the expectation of Eq. (4), and the decay of Eq. (3) is plotted for reference (dashed black).

As expected, as $\rho \rightarrow \infty$, the amplitude decay is more like the far-field distribution of Eq. (3), and as $\rho \rightarrow 0$ the amplitude decay is more like the near-field distribution of Eq. (5). However, since $R=200$ km is neither far-field nor near-field, neither Eq. (3) nor Eq. (5) is obtained even with those extreme values of ρ. Over the range of distances plotted in Fig. 3, the $\rho=0$ distribution has a slope (of the log of the attenuation term) ranging from $3.1 \cdot 10^{-3}$/km to $4.4 \cdot 10^{-3}$/km whereas the $\rho=\infty$ distribution has a slope ranging from $0.2 \cdot 10^{-3}$/km to $1.3 \cdot 10^{-3}$/km (compared with $\alpha=2.0 \cdot 10^{-3}$/km). The intermediate $\rho=3$ distribution has a slope ranging from $1.0 \cdot 10^{-3}$/km to $1.5 \cdot 10^{-3}$/km. We note that $\rho=2$ represents the sum of a uniform distribution and a 200-km far-field distribution of equal strength. Despite the $\rho=3$ distribution thus being 'closer' to (200-km) far-field than uniform, the slopes are always closer to Eq. (4) than Eq. (3), and are approximately halfway between the slope of Eq. (4) ($\rho=1$) and the slope of $\rho=\infty$ over the range plotted. This somewhat higher sensitivity to a uniform source distribution as compared with a far-field source distribution is primarily due to the attenuation of more distant sources, and hence a stronger sensitivity to the more local sources within a given distribution (despite there being many more distant sources). This then implies that even a relatively small amplitude uniform source distribution can potentially overwhelm relatively large amplitude far-field sources, especially if the distance to the far-field sources is relatively large (i.e. $\alpha r_{sx} >> 1$). This observation may explain why noise correlation measurements on the Earth typically have amplitudes that are relatively consistent with those expected based on inferred attenuation coefficients (Lin et al. 2011) despite there likely being a large number of far-field sources (e.g. ocean microseism) compared with local sources (e.g. scattering sources and wind generated noise).

CONCLUSIONS

Using the framework of Tsai (2011), we have calculated the normalized cross correlation (coherency) for a variety of relatively simple noise source distributions. Analytic results show that the decay of amplitudes depends crucially on whether the source distribution is near-field, far-field or uniform. Numerical results for one specific near-field plus far-field case show how the slope of the log of the coherency depends on the relative amplitudes of near-field and far-field terms. The numerical results suggest that far-field sources may not be as important as they might (at first) be expected to be. Thus, as long as researchers can at least roughly estimate the relevant noise source distribution, attenuation measurements should yield robust results.

REFERENCES

Cox, H. [1973]. "Spatial Correlation in Arbitrary Noise Fields with Application to Ambient Sea Noise", J. Acoust. Soc. Am., Vol. 54, pp. 1289-1301.

Harmon, N., C. Rychert, and P. Gerstoft [2010]. "Distribution of Noise Sources for Seismic Interferometry", Geophys. J. Int., Vol. 183, pp. 1470-1484.

Lawrence, J. F., and G. A. Prieto [2011]. "Attenuation Tomography of the Western United States from Ambient Seismic Noise", J. Geophys. Res., Vol. 116, B06302, doi:10.1029/2010JB007836.

Lin, F.-C., M. H. Ritzwoller, and W. Shen [2011]. "On the Reliability of Attenuation Measurements from Ambient Noise Cross-Correlations", Geophys. Res. Lett., Vol. 38, L11303, doi:10.1029/2011GL047366.

Prieto, G. A., J. F. Lawrence, and G. C. Beroza [2009]. "Anelastic Earth Structure from the Coherency of the Ambient Seismic Field", J. Geophys. Res., B07303, doi:10.1029/2008JB006067.

Shapiro, N. M., M. Campillo, L. Stehly, and M. H. Ritzwoller [2005]. "High-Resolution Surface-Wave Tomography from Ambient Seismic Noise", Science, Vol. 307, pp. 1615-1618.

Tsai, V. C. [2009]. "On Establishing the Accuracy of Noise Tomography Travel-Time Measurements in a Realistic Medium", Geophys. J. Int., Vol. 178, pp. 1555-1564.

Tsai, V. C. [2011]. "Understanding the Amplitudes of Noise Correlation Measurements", J. Geophys. Res., in press.